Published in IET Radar, Sonar and Navigation
Received on 25th September 2013
Revised on 17th December 2013
Accepted on 19th January 2014
doi: 10.1049/iet-rsn.2013.0312

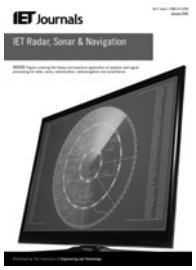

ISSN 1751-8784

Simplistic approach for water vapour sensing using a standalone global positioning system receiver

Saurabh Das, Souvik Majumder, Rohit Chakraborty, Animesh Maitra

Institute of Radio Physics and Electronics, University of Calcutta, 92, A. P. C. Road, Kolkata 700009, India
E-mail: animesh.maitra@gmail.com

Abstract: Precipitable water vapour (PWV) is an important input for numerical weather prediction model, meteorology and high-precision navigational applications. Conventional methods for the determination of PWV using radiosonde are not sufficient owing to poor temporal resolution, whereas radiometer-derived PWV is reliable only in fair weather conditions. Global positioning system (GPS) is a very useful and cost-effective tool to determine PWV continuously in all weather conditions. The processing of GPS data to extract the PWV information is, however, very complicated due to very small effect of the PWV (~0.5% of total delay) on GPS frequencies than other sources of delay and errors and requires a network of GPS in differential configuration for such purpose. The authors show how the problem can be handled in a standalone dual-frequency GPS receiver in a relatively less complicated manner with reasonable accuracy. The performances of different dry tropospheric delay models are also investigated. The methodology is tested with GPS measurements at Kolkata (22.57°N, 88.37°E) and Bangalore (13.01°N, 77.5°E). The results indicate that the proposed methodology can be implemented for PWV estimation using single GPS receiver with satisfactory performance.

1 Introduction

Precipitable water vapour (PWV) is an important input for numerical weather prediction as well as for high-precision navigational applications. It also plays an important role in the propagation of millimetre-wave signal used in communication. However, PWV is highly variable quantity both spatially and temporally. It is difficult to have a single reliable model that can predict PWV in the atmosphere satisfactorily at any given instant of time and place. Hence, the experimental measurement of PWV is of prime importance for meteorology, navigation and communication.

Usually, PWV is estimated using either a radiosonde or a radiometer. The radiosonde estimation of PWV is temporarily very sparse. However, long-term radiosonde data are available that are useful for studying the decadal changes of water vapour [1]. On the other hand, radiometer can provide data with high temporal resolution [2]. But, limited numbers of ground radiometers are presently available because of the cost involved. On the other hand, the space-borne radiometers are not very accurate over the land surfaces even though they have high accuracy over ocean surfaces [3]. Further, the radiometer measurements are reliable only during clear weather conditions.

In this scenario, global positioning system (GPS) is a very useful tool to study the PWV in continuous fashion in all weather conditions [4, 5]. However, the processing of GPS data for such application is an involved process due to the presence of different biases and error sources [6]. The relatively very small magnitude of the wet tropospheric delay (~0.5% of total delay), which is contributed by PWV, is extremely difficult to estimate with high confidence bound [7] in the presence of high amount of errors (ephemeris error ~20%, satellite clock error ~20%, multipath error ~13% and measurement noise ~4%). Further, the ionospheric contribution, especially in the tropical region, is much more dominant (ionospheric delay ~38%) and severe than the tropospheric counterpart (total tropospheric delay ~5%) [4, 8–10].

Usually, differential GPS (DGPS) techniques are employed using a network of GPS receiver for the estimation of PWV. A dense network of GPS dual-frequency receivers is required for PWV estimation with high accuracy. The advantage of such configuration is that the common errors due to clock bias and ephemeris, which are the dominant components, can be eliminated without estimating the same. Similarly, the effect of antenna phase centre and earth crust movements due to tidal effect is also eliminated. The ionospheric part can be tackled using the dual-frequency measurements. However, the factors such as cost and infrastructure involved in such configuration are of practical consideration.

Single receiver can also be used for precise point positioning if all the contributing factors are considered explicitly [6, 11]. Some of the recent papers show the feasibility of using single receiver for PWV estimation by considering precise models of each error sources and biases [12–14]. However, incorporation of all these models results in increase of complexity in the system. Our motivation in this paper is to see (i) whether, in tropical region also, an isolated dual-frequency receiver can give the PWV with reasonable accuracy without employing the DGPS methods and (ii) in less complicated manner. This will be very useful

considering the numbers of GPS receivers presently operating at different regions which are not in a network mode.

In this paper, the technicality and challenges of retrieving PWV from a single GPS receiver have been presented. The effect of various errors on the GPS data and their processing is demonstrated for PWV estimation. The performances of various hydrostatic delay models are then investigated. We have shown that under certain assumptions, PWV with reasonable accuracy can be obtained in a relatively simpler way.

The study used the GPS data obtained from two locations, namely International GPS Service (IGS) station, Bangalore (13.01°N, 77.5°E) and non-IGS station in Kolkata (22.56°N, 88.37°E). The GPS receiver, LEICA GRX1200 with antenna, ATX 1230 is placed at the rooftop of the Institution of Radio Physics and Electronics, University of Calcutta in Kolkata. The receiver Leica GRX1200 has a root mean square (RMS) error of 20 mm in pseudorange measurements, whereas 0.2 mm in carrier phase measurements at both the frequencies [15]. The accuracy in TEC measurements is about 0.2 TECU. The GPS receiver at Bangalore is a part of the IGS reference network. The GPS receiver is ASHTECH UZ-12 with antenna type ASH701945E_M. The ground meteorological data has been collected using Paroscientific MET3A instrument at both the locations. Local radiosonde data at Kolkata and Bangalore are also obtained from India Meteorology Department (IMD). The GPS receiver and the radiosonde launching sites are within ~5 km radius from both the locations. The GPS data have been obtained with 30 s integration time and the meteorological data are obtained with 30 min interval.

The organisation of the paper is as follows: In Section 2, the basic theory of GPS measurement and its relation with the PWV is outlined. The detailed data processing including the discussions of various error sources, its remedy and the assumptions taken here are given in Section 3. Section 4 outlines the estimation procedure of the atmospheric contributions with different tropospheric delay models followed by the results in Section 5.

2 Theory

GPS constellation consists of 24 satellites. Each satellite transmits a uniquely coded data, called pseudo random number (PRN), in two frequencies, L1 (1575.42 MHz) and L2 (1227.6 MHz). Since the intermediate medium between space vehicle (SV) and the receiver is not vacuum, the signal propagation is primarily affected by the ionised particles of the ionosphere and troposphere composed of dry gases and water vapour [6, 9]. However, only the time information of the transmission and reception of the signal is known. Thus, the distance between SV and GPS receiver is approximated by multiplying the time difference with the speed of signal in vacuum. This approximated distance is known as pseudorange (P). Therefore, if one knows the amount of error in the distance estimation, one may get some information about the sources of the errors, that is, about ionosphere and water vapour.

The pseudorange can be written as

$$P = R + (\delta_r - \delta_t)c + R_{iono} + R_{tropo} + \varepsilon \quad (1)$$

Therefore

$$R_{tropo} = P - R - R_{iono} - (\delta_r - \delta_t)c - \varepsilon \quad (2)$$

where R is the geometric range, R_{iono} is ionospheric delay, R_{tropo} is tropospheric delay, δ_r is the receiver clock offset, δ_t is the satellite clock offset and c is the velocity of light. The error, ε, include all the unaccounted and measurements errors.

Equation (2) can be written in matrix form and solved in least square sense for each measurement instants using all available satellites above 15° elevation. This cut off is chosen to reduce the error in measurements due to the multipath effect [6, 9]. Tropospheric delay can be estimated for each satellite link if the values of the parameters on the right hand side of (2) can be modelled properly. The ephemeris and satellite clock corrections can be obtained very precisely using the IGS provided post-process data. The final IGS precise ephemeris and clock information are obtained with a latency of 12–13 days. It is to be noted that the IGS also provide ultra-rapid product of the ephemeris and clock parameters in every 15 min, which may also be used for such purpose [16]. However, we have used the final IGS product as it has better accuracy over the ultra-rapid product. Ionospheric delay is obtained from dual-frequency measurements. The value of R_{tropo} can then be estimated by minimising the error variance of (2) using all visible satellites in least square sense at each measurement instant [17]. For simplicity in the methodology, we have not explicitly used models of parameters like earth–crust movement, tidal effects and antenna phase-centre variations, but remove them without estimating the same using carrier phase smoothening and least-square optimisation technique.

In the following sections, the estimation procedure and pre-processing of the above parameters are discussed in detail.

3 GPS data processing

3.1 Pseudorange pre-processing

The pseudorange is very noisy and erroneous due to the presence of non-synchronous clocks in satellite and receiver. This fact is illustrated in Fig. 1, in which the temporal variation of the difference between pseudorange and geometrical range is plotted to show the effect of non-synchronous clocks. In Fig. 1*a*, the uncorrected pseudorange is used, whereas in Fig. 1*b*, the difference between corrected pseudorange and true range is shown. There is considerable disparity in the results and also a theoretical contradiction is confronted in few cases, when the geometrical range exceeds the pseudorange. We can also note a sinusoidal behaviour of the residual errors, which is mostly due to the multipath effect and depends on the elevation angle. The pseudorange is therefore need to be corrected before use. The first step is to estimate the satellite position accurately for the estimation of the correct geometric range. The SV clock bias as well as the receiver clock offset needs to be estimated next for correcting the pseudorange.

3.1.1 Estimation of satellite co-ordinates: The GPS satellite transmits the navigation message in addition to the observation data. The navigation file contains the ephemeris information about the satellite position in Earth-centred, Earth-fixed coordinate system. The ephemeris data are broadcast for each individual satellite in every two hours and is unique to that individual satellite only. The satellite position can be calculated at the time of transmission of the signal using standard algorithm [9]. But the receiver

doi: 10.1049/iet-rsn.2013.0312

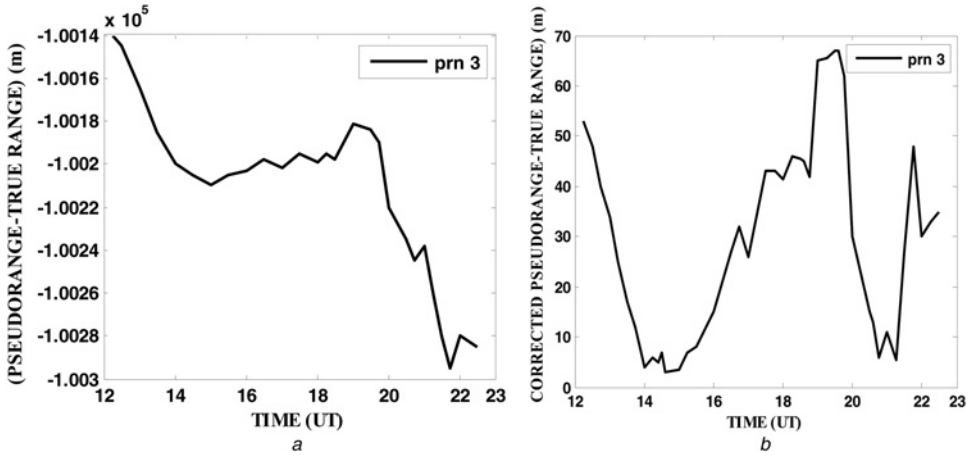

Fig. 1 *Difference between pseudorange and true range with time*
a Before correction
b After correction, 1st January 2010 at Bangalore

position is calculated at the time of signal reception. The satellite moves to a different position by the time the signal is received at the GPS station and this causes some errors in the estimation of R. Hence, the time correction is applied iteratively assuming that the velocity of signal equals to the free-space velocity. In addition, the Doppler effect in the signal due to the relative motion of SV and receiver needs to be taken into account [9, 10]. The transmitted navigation message provides meter-level accuracy in positioning after these corrections. Post-processed data of precise ephemeris are also regularly uploaded in the website (http://www.ngs.noaa.gov), which can further improve the range estimation.

3.1.2 Clock bias: The total clock bias added to the received signal is equal to the satellite clock bias plus receiver clock bias. This arises due to the drifting of satellite clock as well as non-synchronisation of receiver and satellite clocks. The satellite has an atomic clock onboard, whereas the receiver usually uses quartz clock. Therefore, the stability of the receiver clock is very poor and a mismatch between these two clocks occurs. The IGS also provide the satellite clock error information in addition to the precise ephemeris and can be used to correct the satellite clock bias. The final IGS product gives an accuracy of ~75 ps in RMS with standard deviation of ~20 ps in satellite clock estimation whereas the final ephemeris is provided with an accuracy of 2.5 cm (http://igscb.jpl.nasa.gov/components/prods.html).

The clock bias also includes differential P_1P_2 code bias and differential P_2C_1 code bias which are measured separately. The receiver inter-frequency bias arises due to the difference between the frequency response of the filtering and it results in a time-misalignment of the two pseudorange resulting in a systematic bias. Kalman filter technique is generally used to estimate the receiver bias [18]. Differential P_1P_2 code bias can be determined by calculating GPS time offset values and GPS transmitted τ_{GD} values, which are the bias difference between each GPS satellite transmission at two frequencies. They are broadcast on the GPS navigation message so that single-frequency users can use them in conjunction with ionosphere delay estimates, such as, the Klobuchar ionosphere model, to improve their position determination [19].

3.1.3 Transmission time correction: Space vehicle (SV) time is the time of transmission of signal from a SV. The measured time during which the satellite signal reaches the receiver is erroneous due to rotation of the Earth, called the Sagnac effect as well as due to relativistic effect. These effects can be handled by estimating the time delay iteratively assuming free space velocity and by incorporating the SV PRN code phase time offset values [6, 9]. The code offset values are estimated using a polynomial form as follows

$$(\Delta t_{SV})_{L1} = a_{f0} + a_{f1}(t - t_{oc}) + a_{f2}(t - t_{oc})^2 + \Delta t_r + \tau_{GD} \quad (3)$$

where a_{f0}, a_{f1} and a_{f2} are the polynomial coefficients, t_{oc} is the clock data reference time and Δt_r is the relativistic correction term which is given by

$$\Delta t_r = Fe\sqrt{A}\sin(E_k) \quad (4)$$

where Fe is a constant, E_k is the eccentric anomaly and A is the semi-major axis.

3.1.4 Noise and other effects: After the clock corrections, the pseudorange is more reliable but still has various un-modelled noise and effects. Multipath is one of the most important of these un-modelled noise. The movement of earth crust and tidal movement also have an impact on the receiver position [20, 21]. The geometric distance between the antenna phase centres of both the satellites and ground-based receivers also needs to be modelled properly. There exist various methods for such purposes [20] although they are rather complicated. Here, the pseudorange is smoothed and least-square optimisation technique is used [12] to reduce the effect of these parameters on the retrieved ionospheric and tropospheric parameters. This effectively removes the above effects without estimating the same and reduces the complexity of the system.

GPS pseudorange data can be smoothed by carrier phase measurements. Such carrier phase smoothing technique is often referred to as 'carrier phase levelling'. This is done using a moving window of 150 s duration, which has been taken as a tradeoff between the noise suppression efficiency and carrier-code divergence [6]. The carrier phase contains much smaller measurement errors than pseudorange as shown in Fig. 2*a*. In Fig. 2*b*, the smoothed pseudorange difference is shown over the raw pseudorange difference. The dotted line in Fig. 2*a* indicates the plot of $(P_2–C_1)$ in

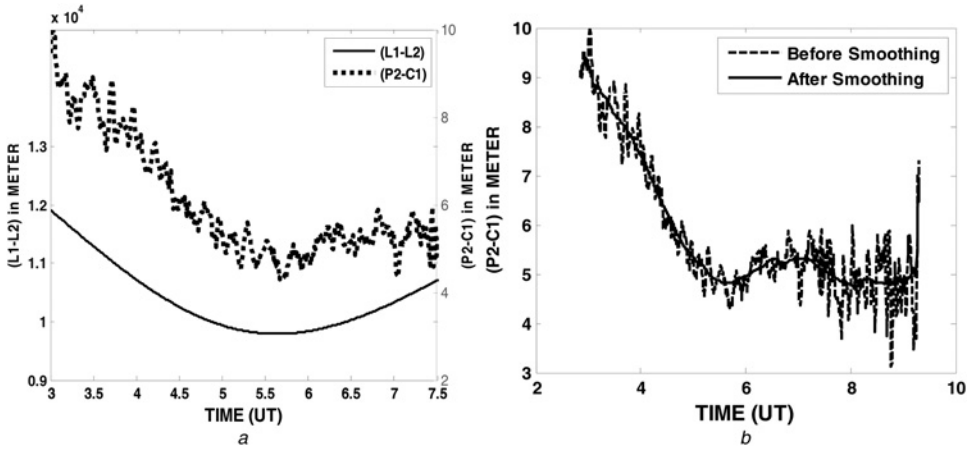

Fig. 2 *Pseudorange data*

a Difference between carrier phases and pseudorange
b Difference between pseudoranges before smoothing and after smoothing for PRN 4 observed from Kolkata on 14th October 2012

metre, which is very noisy and the solid line indicates the plot of $(L_2–L_1)$ in metre, which is quite smooth. So, the pseudorange data were smoothed using carrier phase measurements, as indicated by solid line as shown in Fig. 2*b*.

4 Estimation of atmospheric delays

4.1 Ionospheric delay

The main source of ionospheric delay is due to the electron content of the ionosphere. A measurement of the total electron content (TEC) gives a direct measure of this delay. TEC is defined as the amount of electrons integrated along the ray path from GPS receiver to the SV.

TEC can be obtained as

$$\mathrm{TEC} = \frac{1}{40.3}\frac{f_1^2 f_2^2}{\left(f_1^2 - f_2^2\right)}(P_2 - C_1) \tag{5}$$

GPS carrier phase derived TEC provides smooth but relative measurements of ionospheric TEC as the initial integer ambiguity cannot be resolved [10]. The code-derived TEC measurements, on the other hand, provide a noisy but absolute estimate [6, 9, 10]. Thus, ionospheric TEC can be obtained by carrier phase smoothing of the pseudoranges as shown in Fig. 3. The dotted line indicates the plot of TECs using noisy pseudorange (P_2 and C_1) and solid line indicates the TEC values after carrier phase smoothing.

The typical diurnal variations of vertical TEC (VTEC) as observed at Bangalore and Kolkata are shown in Fig. 4.

The estimated VTEC can now yield the ionospheric delay, R_{iono}. To obtain an idea of the nature of this delay, a time series of the variation in R_{iono} is presented for the same dates as shown in Fig. 5 for both the locations. We can note that the maximum zenith delay as well as the VTEC occurs during local noon time, that is, around 0930 UTC, as expected. However, since Kolkata is situated at the northern crest of ionospheric anomaly region [22], the zenith delay is higher (~14 m) than the equatorial region of Bangalore (~7 m).

4.2 Tropospheric delay

We can now estimate the delay due to the tropospheric parameters using (2). The tropospheric delay has two components, namely, hydrostatic or dry component and a wet component. The hydrostatic component in zenith direction is called zenith hydrostatic delay (ZHD). It can be estimated from surface pressure measurements. The zenith wet delay (ZWD), caused by the PWV, cannot be sufficiently modelled by surface measurements due to the varying distribution of water vapour in the atmosphere [6, 9, 10].

At a particular time, different GPS satellites are visible at different elevation angles. The delay associated with these satellites is termed as slant total delay. The slant total delays are then mapped to zenith direction using a suitable mapping function since hydrostatic delay models can give values only in the zenith direction [6, 9, 10].

The slant total delay is expressed as

$$\mathrm{STD}(\varepsilon) = \mathrm{mf_h}(\varepsilon)\mathrm{ZHD} + \mathrm{mf_w}(\varepsilon)\mathrm{ZWD} \tag{6}$$

where ε is the elevation angle of the GPS satellites, $\mathrm{mf_h}$ is the dry mapping function and $\mathrm{mf_w}$ is the wet mapping function.

Here, we have used Niell mapping function [8] with separate coefficients for hydrostatic and wet delay. It is to be noted that there exist various other mapping functions for such conversion. We used the Niell mapping function because of its simplicity and satisfactory performance reported in the open literatures [23].

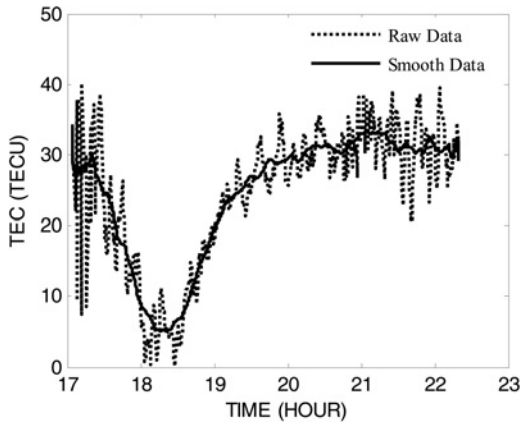

Fig. 3 *TEC before and after smoothing with time for PRN 8 at Kolkata on 1st April 2013*

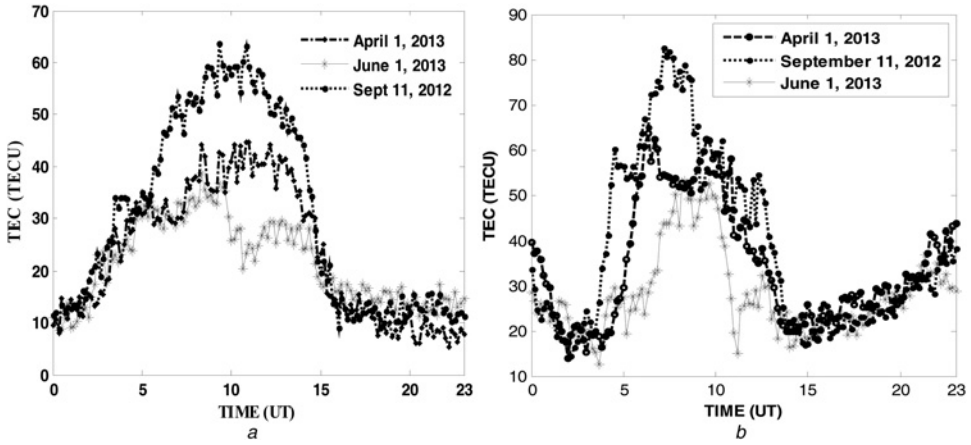

Fig. 4 *VTEC*
a Bangalore
b Kolkata

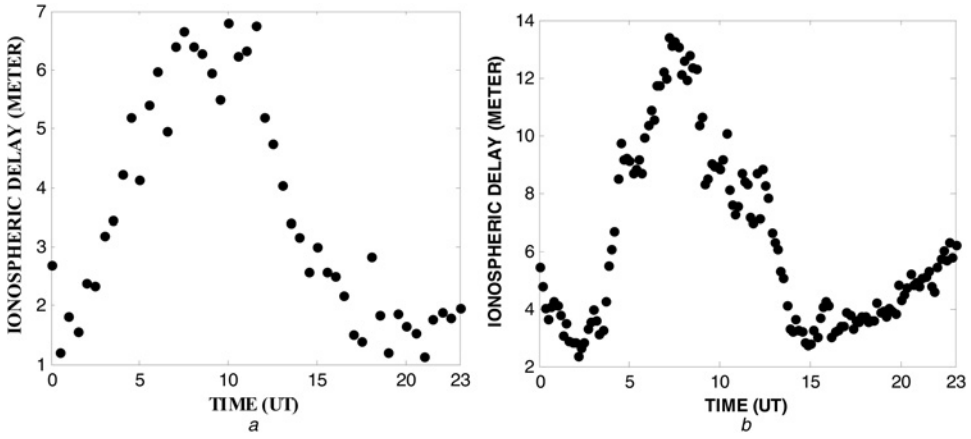

Fig. 5 *Ionospheric delay at L1 frequency*
a Bangalore on 1st January 2010
b At Kolkata on 1st April 2013

4.3 Hydrostatic delay models

The hydrostatic delay is the major contributor of the total GPS signal delay in the troposphere. It can be estimated using various models [12, 24]. The tropospheric model developed by University of New Brunswick (UNB) and Radio Technical Commission for Aeronautics (RTCA) model used by wide area augmentation system (WAAS) incorporate latitudinal variation in the delay [25]. However, since the RTCA model uses the US atmospheric data, the performance of the same over Indian region is yet to be ascertained [26]. Further, previous studies indicate that the conventional models, like Hopfeild and Saastamoinen, perform better than the WAAS model [27]. Accordingly, we have tested the following three models to identify the suitability over Indian region as given in the following sections.

4.3.1 Hopfield model: According to this model, ZHD can be expressed [6, 9] as

$$\text{ZHD} = 1.552(h - H)\frac{P}{T} \tag{7}$$

where

$$h = 40.082 + 0.14898(T - 273.16)$$

H is the height of station above sea level (km), T is the surface temperature (K) and P is the surface pressure (hPa).

4.3.2 Saastamoinen model: According to this model, ZHD can be expressed [28, 29] as

$$\text{ZHD} = \frac{0.00227768}{f(\lambda,\ h)}P \tag{8}$$

where

$$f(\lambda,\ h) = (1 - 0.00266\cos(2\Phi) - 0.00028h_{\text{ref}}) \tag{9}$$

ϕ is the latitude of the site (in radians) and h_{ref} is the site height (in km) above the geoid.

The basic advantage of Saastamoinen model over Hopfield model is that no temperature measurements are needed here [28, 29]. The height of the station and its latitude are used for the computation of the gravity correction.

4.3.3 Black model: According to this model, ZHD can be expressed [6, 9] as

$$\text{ZHD} = 0.2343(T - 4.12)\frac{P}{T} \tag{10}$$

4.4 Wet delay

Theoretically, ZWD can be obtained as

$$\mathrm{ZWD} = 10^{-6}\left(k_2' \int \frac{P_\mathrm{v}}{T}\mathrm{d}z + k_3 \int \frac{P_\mathrm{v}}{T^2}\mathrm{d}z\right) \tag{11}$$

where $k_2' = (17 \pm 10)$ K mb^{-1}, $k_3 = (3.776 \pm 0.004) \times 10^5$ K^2 mb^{-1} and P_v is the partial pressure of water vapour.

Since the integral of the partial pressure cannot be measured at every point with sufficient accuracy, the estimated ZWD will not be very accurate. It is easier to measure the total delay from GPS measurements, and then correct it using the reliable hydrostatic delay obtained from the ground level measurements. The remaining portion of total delay is wet delay.

Once a wet delay is determined, it can then be mathematically converted into total PWV [4] as follows

$$\mathrm{PWV} = \frac{\mathrm{ZWD}}{K} \tag{12}$$

where K is dimensionless and given by

$$K = \left[10^{-6}\left(\frac{k_3}{T_m} + k_2'\right)R_\mathrm{v}\rho\right] \tag{13}$$

$$T_m = 55.8 + 0.77 \times T \tag{14}$$

where ρ is the density of water in kg/m^3 and R_v is water vapour gas constant (4.615×10^2 J/Kg/K).

5 Results

5.1 Comparison among different hydrostatic models

Three models, as discussed in Section 4, were used to calculate the ZHD from ground meteorological data [12]. ZWD as well as PWV are then calculated by subtracting the ZHD from the total tropospheric delay measured by GPS. The comparison of the estimated PWV for Bangalore is shown in Fig. 6 using these three hydrostatics delay models.

We can see that the Hopfield and Saastamoinen (SAAS) models give almost the same values of PWV but the Black model provides relatively lower value. The advantage of using SAAS model is that it is independent of the temperature but Hopfield and Black models are influenced by errors in the temperature measurement. Therefore, in our approach, we used SAAS model to avoid the temperature dependence. Similar observations are also reported by Mendes [27].

5.2 Comparison of estimated PWV with radiosonde

To validate the PWV measured by our system, we compared it with local radiosonde data. PWV can be estimated from radiosonde data indirectly. The value of PWV can be computed by integrating specific humidity (q) for the whole

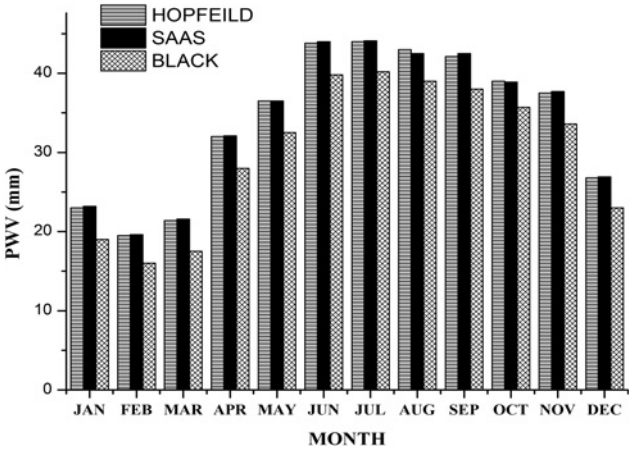

Fig. 6 *Comparing PWV for different models at Bangalore in the year 2010*

atmospheric height [30]. This is expressed as

$$\mathrm{PWV} = \frac{1}{g\int_0^p q\,\mathrm{d}p} \tag{15}$$

$$\mathrm{PWV} = \frac{1}{2g\sum_{i-1}^{n-1}(q_i + q_{i+1}) \times (P_i - P_{i+1})} \tag{16}$$

where g is the acceleration due to gravity. The relationship between q and mixing ratio (α) is given below

$$q = \frac{\alpha}{\alpha + 1} \tag{17}$$

Since radiosonde data can only be obtained twice a day, we have calculated the PWV values from radiosonde and validated it with that obtained from GPS output for the same time. The GPS measured values are averaged over 10 min around the time of radiosonde launching. The GPS data and radiosonde data for Bangalore are compared on monthly basis for year 2009 as shown in Fig. 7.

We can see a prominent seasonal pattern of water vapour, which is consistent with the atmospheric conditions. The comparison with radiosonde data shows good agreement for most of the months. The limited mismatch between

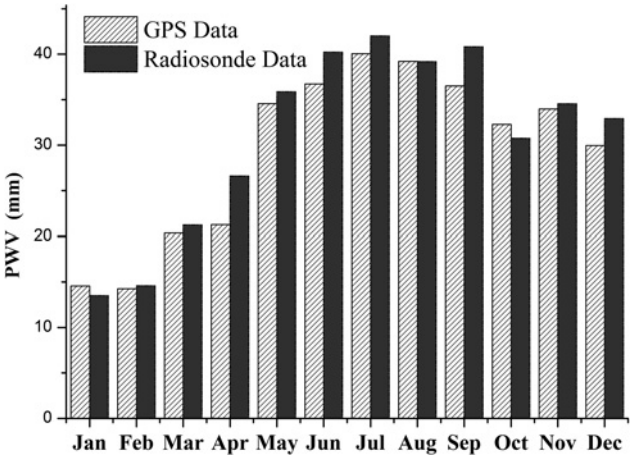

Fig. 7 *Monthly mean PWV values as obtained from GPS and radiosonde at Bangalore for the year 2009*

doi: 10.1049/iet-rsn.2013.0312

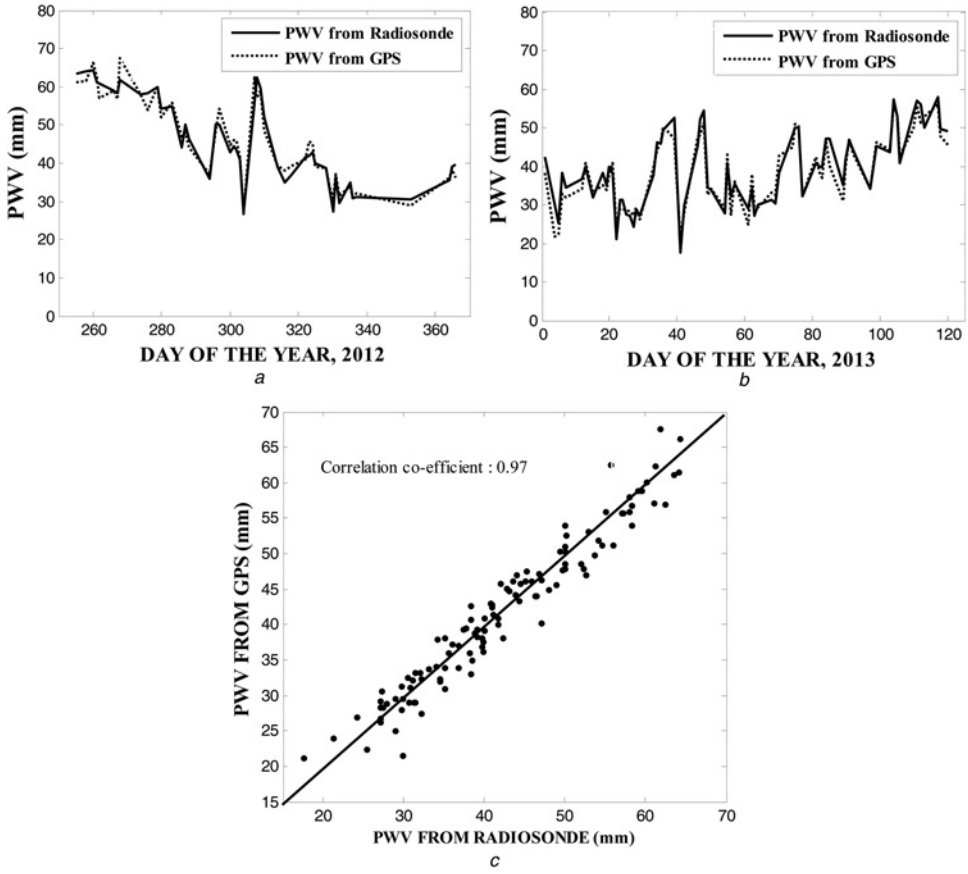

Fig. 8 *Comparison of GPS derived PWV at Kolkata with radiosonde*

a Time series plot of 2012
b Time series plot of 2013
c Scatter plot (combined 2012 and 2013)

radiosonde observations and estimated PWV values may be due to the errors in retrieval method and/or due to the spatial variability of PWV. It is to be noted that since the GPS receiver and radiosonde are not exactly collocated, the difference in PWV at both the locations may also introduce some error.

In Fig. 8, a comparison of radiosonde observations with GPS measurements taken at Kolkata is shown. Since we do not have a full-year measurement, we analyse the correlation between the observed value and the computed value with 117 samples. This result also indicates that our methodology performs satisfactorily.

From Figs. 8*a* and *b*, we can see that the variations in PWV obtained from both the instrument is matched very well for both the year 2012 and 2013. In Fig. 8*c*, the scatter plot between the PWV from both the instruments also indicates a good correlation (0.97) between them.

The distribution of percentage errors between radiosonde data and retrieved PWV is shown in Fig. 9. Since we took the radiosonde data as the truth data, the percentages is calculated with reference to the radiosonde data. It can be seen from Fig. 9 that the errors have a zero mean and >80% of data points are within the error range of ±5%. This also indicates that no significant bias is present in the retrieval method.

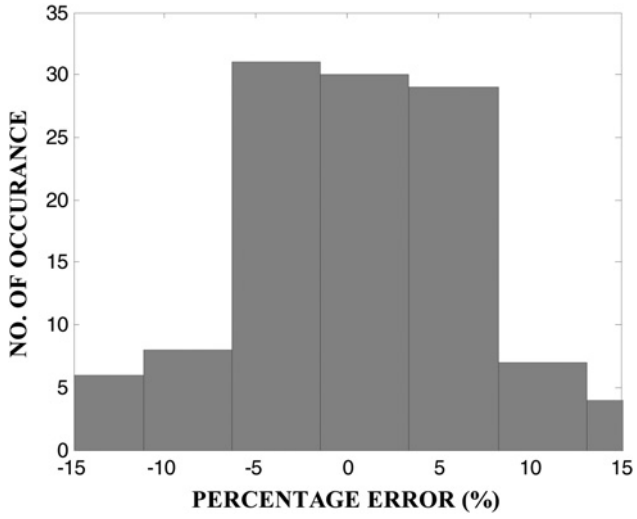

Fig. 9 *Percentage distribution of errors*

6 Discussion and conclusion

The estimation of PWV from single GPS receiver measurements provides opportunity to monitor the atmospheric parameter with a less involved system in all weather conditions and in a continuous fashion. However, the processing of raw GPS data for such purposes is a complex process, especially for the isolated GPS receiver. In this paper, we present a simplistic approach to estimate the PWV from GPS measurement with reasonable accuracy. The effect of different biases on GPS signal and removal of such biases are discussed in detail. The estimation of TEC

is also discussed. The errors are minimised in our data processing by smoothening of the pseudorange data and using least-square optimisation technique. We observe that the methodology as detailed above can provide good results in comparison to the radiosonde measurements in short term as well as long-term basis.

We have observed that the dry component of the tropospheric delay can be modelled with reasonable matching with various algorithms. However, we have employed the Saastamoinen model in our approach to avoid the temperature dependence. The results indicate that the above technique will reduce the complexity in PWV estimation greatly and can still be able to give the PWV values from isolated single receiver. The finding will be helpful in obtaining PWV from large number of receivers currently operating worldwide in singular mode and beneficial for many applications where very high accuracy of instantaneous PWV is not required. In future, we have a plan to improve our algorithm for near real-time estimation of PWV using the IGS provided ultra-rapid ephemeris and clock data.

7 Acknowledgment

The financial support provided by ISRO under the projects (i) 'Integrated studies on water vapour liquid water content and rain of tropospheric atmosphere and effects in radio environment', (ii) 'Space Science Promotion Scheme' and (iii) 'TEQUIP Phase-II' are thankfully acknowledged. The authors also acknowledge the effort in data collection by IGS, Bangalore station.

8 References

1 Liu, Y., Chen, Y., Baki, Iz, H.: 'Precision of precipitable water vapor from radiosonde data for GPS solutions', *Geomatica*, 2000, **54**, (2), pp. 171–175
2 Guiraud, F.O., Howard, J., Hogg, D.C.: 'A dual-channel microwave radiometer for measurement of precipitable water vapor and liquid', *IEEE Trans. Geosci. Electron.*, 1979, **17**, (4), pp. 129–136
3 Hanssen, R.F., Feijt, A.J., Bilt, D., Klees, R.: 'Comparison of precipitable water vapor observations by spaceborne radar interferometry and meteosat 6.7-μm radiometry', *J. Atmosph. Ocean. Technol.*, 2001, **18**, pp. 756–764
4 Jade, S., Vijayan, M.S.M.: 'GPS based atmospheric precipitable water vapor estimation using meteorological parameter interpolated from NCEP global reanalyzed data', *J. Geophys. Res.*, 2008, **113**, pp. D03106
5 Suparta, W.: 'Variability of GPS and precipitable water vapor over Antarctica comparison between observed and predicted', *World Appl. Sci. J.*, **12**, (9), 2011, pp. 1597–1604
6 Misra, P., Enge, P.: 'Global positioning system: signals, measurements, and performance' (Ganga-Jamuna Press, 2006, 2nd edn.)
7 Skone, S., Hoyle, V.: 'Troposphere modelling in a regional GPS network', *J. Global Position. Syst.*, 2005, **4**, (1–2), pp. 230–239
8 Niell, A.E.: 'Global mapping functions for the atmosphere delay at radio wavelengths', *J. Geophys. Res.*, 1996, **101**, pp. 3227–3247
9 Kaplan, E.D., Hegarty, C.J.: 'Understanding GPS: principles and applications' (Artech House, 2006, 2nd edn.)
10 Parkinson, B.W., Enge, P.K., Spilker, J.J.: 'Differential GPS. In global positioning system: theory and applications', *Am. Inst. Aeronaut. Astronaut.*, 1996, **II**, pp. 3–115
11 Kouba, J., Héroux, P.: 'Precise point positioning using IGS orbit and clock products', *GPS Solution*, 2001, **5**, (2), pp. 12–28
12 Zhu, Q., Zhao, Z., Lin, L.: 'Real time estimation of slant path tropospheric delay at very low elevation based on singular ground-based global positioning system station', *IET Radar Sonar Navig.*, 2013, **7**, (7), pp. 7–11
13 Lin, L.K., Zhao, Z.W., Zhu, Q.L.: 'Profiling tropospheric refractivity in real time, based on a relevance vector machine and single ground-based GPS receiver', *Int. J. Remote Sens.*, 2012, **33**, (13), pp. 4044–4058
14 Lin, L.K., Zhao, Z.W., Zhang, Y.R.: 'Tropospheric refractivity profiling based on refractivity profile model using single ground-based global positioning system', *IET Radar Sonar Navig.*, 2011, **5**, (1), pp. 7–11
15 Takac, F., Walford, J.: 'Leica system 1200-high performance GNSS technology for RTK applications'. Proc. 19th Int. Technical Meeting of the Satellite Division of the Institute of Navigation, Fort Worth, Texas, September 2006, pp. 217–225
16 Choi, K.K., Ray, J., Griffiths, J., Bae, T.: 'Evaluation of GPS orbit prediction strategies for the IGS ultra-rapid products', *GPS Solution*, 2013, **17**, (3), pp. 403–412
17 Lowry, A.R., Rocken, C., Sokolovskiy, S.V., Anderson, K.D.: 'Vertical profiling of atmospheric refractivity from ground-based GPS', *Radio Sci.*, 2002, **37**, (3), pp. 1041–1059, doi: 10.1029/2000RS002565
18 Sardon, E., Rius, A., Zarroa, N.: 'Estimation of the transmitter and receiver differential biases and the ionospheric total electron content from GPS observations', *Radio Sci.*, 1994, **29**, pp. 577
19 Klobuchar, J.A., Parkinson, B.W., Spilker, J.J.: 'Ionospheric effect on GPS in global positioning system: theory and applications', *Am. Inst. Aeronaut. Astronaut.*, 1996, **1**, pp. 513–514
20 Blewitt, L.G.D., Clarke, P., Nurutdinov, K.: 'A new global mode of earth deformation: seasonal cycle detected', *Science*, 2001, **294**, pp. 2342–2345
21 Wahr, J.M.: 'The forced nutation of an elliptical, rotating, elastic, and ocean less earth', *Geophys. J. R. Astronaut. Soc.*, 1981, **64**, pp. 705–727
22 Rama Rao, P.V.S., Gopi Krishna, S., Niranjan, K., Prasad, D.S.V.V.D.: 'Temporal and spatial variations in TEC using simultaneous measurements from the Indian GPS network of receivers during the low solar activity period of 2004–2005', *Ann. Geophys.*, 2006, **24**, pp. 3279–3292
23 Boehm, J., Niell, A., Tregoning, P., Shuh, H.: 'Global mapping function (GMF): a new empirical mapping function base on numerical weather model data', *Geophys. Res. Lett.*, 2006, **33**, pp. L07304
24 Liu, Y., Bâki Iz, H., Chen, Y.: 'Calibration of zenith hydrostatic delay model for local GPS applications', *Radio Sci.*, 2000, **35**, (1), pp. 133–140
25 Leandro, R., Santos, M., Langley, R.B.: 'UNB neutral atmosphere models: development and performance' Proceedings of the Institute of Navigation National Technical Meeting, 2006, pp. 564–573
26 Parameswaran, K., Raju, C.S., Saha, K., Ravindran, S.: 'Region-specific tropospheric delay model for the Indian subcontinent'. Space Physics Laboratory, VSSC, Trivandrum, ICG-Meeting, 2007
27 Mendes, V.B.: 'Modeling the neutral-atmosphere propagation delay in radiometric space techniques'. PhD dissertation, Department of Geodesy and Geomatics Engineering Technical Report No. 199, University of New Brunswick, Fredericton, New Brunswick, Canada, 1999, p. 353
28 Bai, Z., Feng, Y.: 'GPS water vapor estimation using interpolated surface meteorological data from Australian automatic weather stations', *J. Global Position. Syst.*, 2003, **2**, (2), pp. 83–89
29 Saastamoinen, J.: 'Atmospheric correction for the troposphere and stratosphere in radio ranging of satellites, in the use of artificial satellites for geodesy', *Geophys. Monogr. Ser.*, 1972, **15**, pp. 247–251 (edited by S. W. Henriksen, A. Mancini, and B.H. Chovitz, AGU, Washington, DC)
30 Prakash, S., Giri, R.K., Adesh: 'Precipitable water vapour at Santa Cruz airport Mumbai from radiosonde measurements: a study', *Int. J. Phys. Math. Sci.*, 2012, **2**, (1), pp. 120–130